

**Innovations Deserving
Exploratory Analysis Programs**

Safety IDEA Program

Development of a Diagnostic System for Air Brakes in Trucks

Final Report for
Safety IDEA Project 12

Prepared by:
Swaroop Dharba and K.R. Rajagopal
Texas A&M University
College Station, TX

August 2008

TRANSPORTATION RESEARCH BOARD
OF THE NATIONAL ACADEMIES

INNOVATIONS DESERVING EXPLORATORY ANALYSIS (IDEA) PROGRAMS MANAGED BY THE TRANSPORTATION RESEARCH BOARD

This Safety IDEA project was funded by the Safety IDEA Program, which focuses on innovative approaches for improving railroad safety and intercity bus and truck safety. The Safety IDEA Program is funded by the Federal Motor Carrier Safety Administration (FMCSA) and the Federal Railroad Administration (FRA) of the U.S. Department of Transportation. Any opinions, findings, conclusions, or recommendations expressed in this publication are those of the authors and do not necessarily reflect the views of the sponsors of the Safety IDEA program.

The Safety IDEA Program is one of four IDEA programs managed by TRB. The other IDEA programs are listed below.

- The Transit IDEA Program, which supports development and testing of innovative concepts and methods for advancing transit practice, is funded by the Federal Transit Administration (FTA) as part of the Transit Cooperative Research Program (TCRP).
- The NCHRP Highway IDEA Program, which focuses on advances in the design, construction, and maintenance of highway systems, is part of the National Cooperative Highway Research Program (NCHRP).
- The High-Speed Rail IDEA Program, which focuses on innovative methods and technology in support of the next-generation high-speed rail technology development program, is funded by the FRA.

Management of the four IDEA programs is coordinated to promote the development and testing of innovative concepts, methods, and technologies for these areas of surface transportation.

For information on the IDEA programs, look on the Internet at www.trb.org/idea, or contact the IDEA programs office by telephone at (202) 334-3310 or by fax at (202) 334-3471.

IDEA Programs
Transportation Research Board
500 Fifth Street, NW
Washington, DC 20001

The project that is the subject of this contractor-authored report was a part of the Innovations Deserving Exploratory Analysis (IDEA) Programs, which are managed by the Transportation Research Board (TRB) with the approval of the Governing Board of the National Research Council. The members of the oversight committee that monitored the project and reviewed the report were chosen for their special competencies and with regard for appropriate balance. The views expressed in this report are those of the contractor who conducted the investigation documented in this report and do not necessarily reflect those of the Transportation Research Board, the National Research Council, or the sponsors of the IDEA Programs. This document has not been edited by TRB.

The Transportation Research Board of the National Academies, the National Research Council, and the organizations that sponsor the IDEA Programs do not endorse products or manufacturers. Trade or manufacturers' names appear herein solely because they are considered essential to the object of the investigation.

Development of a Diagnostic System for Air Brakes in Trucks

Draft Final Report
Safety IDEA Project 12

Prepared for
Safety IDEA Program
Transportation Research Board
National Research Council

Prepared by
Dr. Swaroop Darbha and Dr. K.R. Rajagopal
Texas Transportation Institution
Texas A&M University
College Station, TX

August 2008

Expert Review Panel Members

This SAFETY IDEA project has been guided and reviewed by the members of the expert review panel. Following are the members of the expert review panel:

1. Mr. Alan Korn, Chief Engineer, Meritor-WABCO Truck Brake Systems, Troy, MI.
2. Dr. Rajesh Rajamani, Professor, Department of Mechanical Engineering, University of Minnesota, Minneapolis, MN.
3. Dr. Giorgio Rizzoni, The Ford Motor Company Chair of Electromechanical Systems, Professor of Mechanical and Electrical Engineering, Ohio State University, Columbus, OH.
4. Dr. Karl Hedrick, James Marshall Wells Professor of Mechanical Engineering, University of California, Berkeley, CA.

Contents

Executive Summary	1
1. Introduction	2
2. Experimental setup	3
3. Model of the Pneumatic Subsystem	8
4. Modeling Pressure transients in the Presence of Leak	12
4.1 Derivation of \dot{m}_{leak}	12
4.2 Estimation of effective leak area	13
4.3 Experimental procedure	14
4.3.1 Corroboration of measurements	14
4.3.2 Leak measurements	15
4.4 Corroboration of the mathematical model in the presence of leaks	16
4.5 Realistic leaks	19
5. Push rod stroke estimation	20
5.1 Estimation of the push rod stroke by discretization of the possible range of values:	20
5.2 Scheme 2 – detection of the transition from mode 2 to mode 3	23
5.3 Results at 90 psi supply under no leak conditions	24
5.4 Push rod stroke estimation in the presence of a leak	25
6. Conclusions	29
7. Investigator Profile	30
References	31

List of Figures

1. A general layout of commercial vehicles air brake system	3
2. S-cam foundation brake.	4
3. Test setup at Texas A&M University.	5
4. Schematic of the leak measurement test setup.	6
5. Flow Control Valve (FCV).	6
6. Velocity transducer.	7
7. Leak measurement setup.	7
8. Experimental setup.	8
9. Sectional view of the brake chamber.	9
10. Calibration curve at 653kPa (80 psig) supply pressure.	9
11. Pressure transients at 90psig supply.	11
12. Leak flow rates at various supply pressures and FCV settings.	12
13. Schematic of the setup for leak corroboration tests.	14
14. Comparison of measured and predicted mass values at two turns of FCV.	15
15. Pressure transients at 90 psi supply and 0.5 turns of FCV.	17
16. Pressure transients at 90 psi supply and 1 turn of FCV.	17
17. Pressure transients at 90 psi supply and 2 turns of FCV.	18
18. Pressure transients at 90 psi supply and 2.5 turns of FCV.	18
19. Pressure transients at 90 psi supply with 1.4mm orifice.	19
20. Normalized pressure residue at 653 kPa (80 psig) supply pressure	22
21. Normalized pressure residue at 722 kPa (90 psig) supply pressure	22
22. Error Mode–II&III Pct=1.52 bar	24
23. Error Mode –II&III Pct = 1.57 bar	24
24. Transition detection at 722 kPa (90 psig) supply pressure	25
25. Error in Mode-II & III for 90 psig supply (FCV ¼ open)	26
26. Transition detection at 722 kPa (90 psig) supply pressure (FCV ¼ open)	26
27. Error in Mode-II & III for 80 psig supply(FCV ¼ open)	27
28. Transition detection at 722 kPa (90 psig) supply pressure (FCV ¼ open)	27

List of Tables

1. Leak mass flow rates for a full brake application at 90 psi supply pressure	15
2. Leak mass flow rates for a full brake application at 80 psi supply pressure	16
3. Estimates of K and effective leak area	16
4. Comparison of model and measured steady state pressures	17
5. Estimates of K and effective leak area for the orifices	19
6. Comparison of the Actual and the Estimated Push Rod Stroke	25
7. Comparison of the Actual and the Estimated Push Rod Stroke (with leak)	28

Executive Summary

The purpose of this project was to enhance the safety of trucks by developing diagnostic systems that assess the health of brake systems. Brake systems in trucks are crucial for ensuring the safety of vehicles and passengers on the roadways. Most trucks in the US are equipped with S-cam air brake systems and they are sensitive to maintenance. Moreover, any incident involving trucks results in material damage, which can have serious environmental and economic repercussions, and sometimes, the loss of life, which cannot be measured in economic terms.

This project consisted of three stages. In the first stage, we developed leak detection algorithms based on a mathematical model that predicts the evolution of the pressure in the brake chambers, without leak, in response to the brake pedal input. This leak detection algorithm was based on comparing the measured and observed steady state pressures in the brake chamber at supply pressures indicated by the Federal Motor Vehicle Safety Standards at full brake application. We introduced an audible leak by loosening the couplings for the purposes of experiments. We found out that such leaks did result in a significant drop in the measured brake pressure when compared with the supply pressure as well as the predicted brake pressure.

The second stage included the estimation of push rod stroke in the absence of a leak. Push rod stroke of a brake chamber was found to be dependent on the steady state brake chamber pressure and the pressure when brake pads contact the drum. The estimation scheme involved simultaneously solving the governing equations at various values of pushrod stroke and determining the value for which the predicted and measured brake pressure responses match closely. This estimate compares favorably with the measured value of pushrod stroke under full braking conditions.

The third stage included the development, experimental implementation, testing and evaluation of the prototype diagnostic system in the presence of leaks. The prototype diagnostic system performed two tasks – to estimate the severity of leaks and estimate the pushrod stroke in the presence of leaks. The prototype diagnostic system consisted of a data-acquisition system which interfaces with the truck brake system test bench in the laboratory at Texas A&M University and a desktop computer.

Tests of the prototype diagnostic system conducted on the test bench at Texas A&M University indicated that the prototype diagnostic system accurately predicts the “severity” of the leak (characterized by the “effective area” of the cross-section of the leak) and reasonably predicts the pushrod stroke in the presence of leaks. The underlying algorithms required the development and corroboration of a mathematical model for pressure transients in the presence of a leak. The model used orifice equations for describing the mass flow rate of air leaking and incorporated the balance of mass equation. Experiments indicate that the resulting mathematical model successfully predicts brake pressure.

1. Introduction

The purpose of this project was to enhance the safety of trucks by developing diagnostic systems that assess the health of a brake system. Brake systems in trucks are crucial for ensuring the safety of vehicles and passengers on the roadways. Most trucks in the US are equipped with S-cam air brake systems and they are sensitive to maintenance. Moreover, any incident involving trucks results in material damage, which can have serious environmental and economic repercussions, and sometimes, the loss of life, which cannot be measured in economic terms. It has been reported in the literature that defects in the operation of a brake system in trucks is a significant contributor to accidents and vehicles being put out of service.

This project consisted of three stages. The first stage dealt with the development of leak detection algorithms. The algorithms were based on a mathematical model that predicted the evolution of the pressure in the brake chambers in the absence of any leaks in the system. This was achieved by comparing the measured and predicted steady state pressures in the brake chamber at supply pressures indicated by the Federal Motor Vehicle Safety Standards at full brake application.

The second stage included the estimation of the pushrod stroke when there is no leak in the system. The estimation scheme is based on an experimentally found correlation between pushrod stroke, brake pad contact pressure and the steady-state pressure in the brake chamber. In this scheme, the possible values of pushrod stroke are discretized and the pressure in the brake chamber is predicted using the developed mathematical model, which has pushrod stroke as a parameter. The scheme then determines the best value among the discretized values of pushrod stroke for which the measured and predicted pressure in the brake chamber is close. The estimated push-rod stroke without leak model agreed closely with the measured push rod strokes.

The final stage included the development, experimental implementation, testing and evaluation of a prototype diagnostic for a truck brake system in the presence of leaks. The prototype system consisted of an experimental test bench at Texas A&M University, a data acquisition system, pressure and pedal position sensors, a desktop computer. The purpose of the final stage of the project was to estimate the severity of a leak and then estimate the pushrod stroke in the presence of a leak. The diagnostic algorithms required the development of a mathematical model for pressure transients in the brake chamber in the presence of a leak. In order to corroborate the mathematical model, mass rate of air leaking from the experimental setup was compared with the mass rate of air computed from an "orifice" model for the leak. The "no-leak" model is based on the balance of mass equation and this equation was modified to take into account the mass rate of air leaking as a function of the size of the leak. With this modification, the measured and predicted values of brake pressure agreed closely in the presence of a leak. This model was then used to develop and successfully implement schemes for estimating the severity of the leak in the brake system as well as for estimating the pushrod stroke in the presence of leaks on the experimental setup at Texas A&M University.

2. Experimental setup

A layout of the air brake system found in a typical truck tractor is presented in Fig. 1. An engine-driven air compressor is used to compress air and the compressed air is collected in storage reservoirs. A governor serves to control the pressure of the compressed air stored in the reservoirs. This compressed air is transmitted from the reservoirs to the supply port of a treadle valve. The driver applies the brake by pressing the brake pedal on the treadle valve. This action meters out the compressed air from the supply port of the treadle valve to its delivery port. Compressed air travels from the delivery port of the treadle valve through air hoses to the brake chambers mounted on the axles.

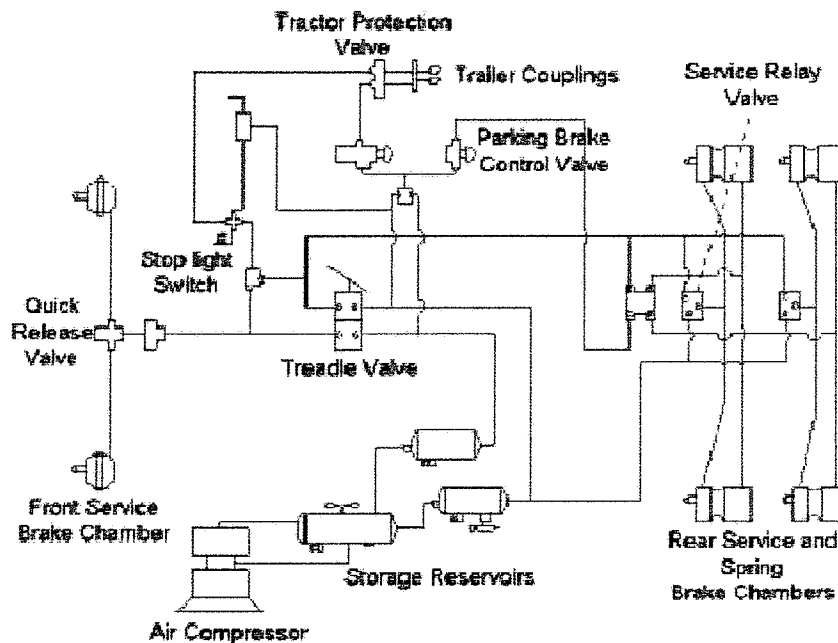


FIGURE 1: A general layout of commercial vehicles air brake system.

The S-cam foundation brake, found in more than 85% of the air-braked vehicles in the United States [1], is shown in Fig. 2. Compressed air from the treadle valve enters the brake chamber and acts against the diaphragm generating a force resulting in the motion of the push rod. The motion of the push rod serves to rotate, through the slack adjuster, a splined shaft on which a cam in the shape of an S is mounted. The ends of two brake shoes rest on the profile of the S-cam and the rotation of the S-cam pushes the brake shoes outwards so that the brake pads make contact with the rotating drum. This action results in the deceleration of the rotating drum. When the brake pedal is released by the driver, the push rod strokes back into the brake chamber and the S-cam rotates in the opposite direction. The contact between the brake pads and the drum is now broken and the brake is thus released.

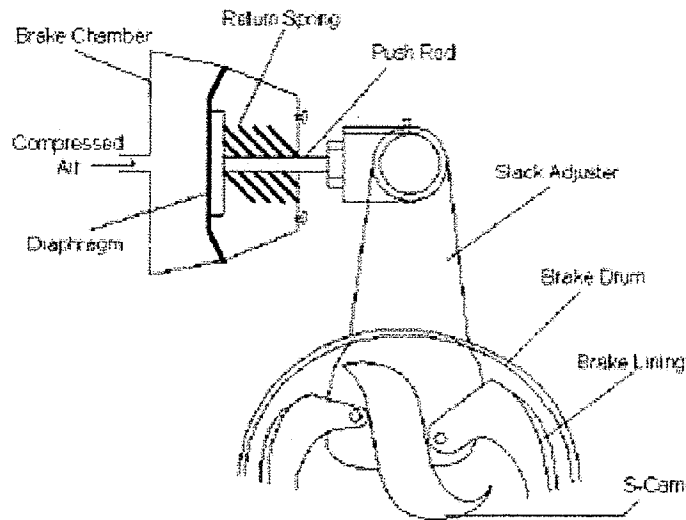


FIGURE 2: S-cam foundation brake.

A photograph of the experimental setup at Texas A& M University is provided in Fig. 3. Two Type-20 brake chambers (having an effective cross-sectional area of 20 in²) are mounted on a front axle of a tractor and two Type-30 (having an effective cross-sectional area of 30 in²) are mounted on a fixture designed to simulate the rear axle of a tractor. It is interesting to note that prior to the 1980s, drivers used to disconnect the front wheel brakes of their vehicle in order to obtain better control during braking. But subsequently tremendous improvements have been made in the design of the vehicle and a federal law passed in January 1987 requires that the brakes be operational on all the wheels of a commercial vehicle [2].

The air supply to the system is provided by means of two compressors and storage reservoirs. The reservoirs are chosen such that their volume is more than twelve times the volume of the brake chambers that they provide to, as required by the Federal Motor Vehicle Safety Standards 121 (FMVSS 121) [3].

Pressure regulators are mounted at the delivery ports of the reservoir to control the supply pressure to the treadle valve. The treadle valve consists of two circuits - the primary circuit and the secondary circuit. The delivery port of the primary circuit is connected to the control port of the relay valve and the delivery ports of the relay valve are connected to the two rear brake chambers. The relay valve has a separate port for obtaining compressed air supply from the reservoir. The delivery port of the secondary circuit is connected to the Quick Release Valve (QRV) and the delivery ports of the QRV are connected to the two front brake chambers.

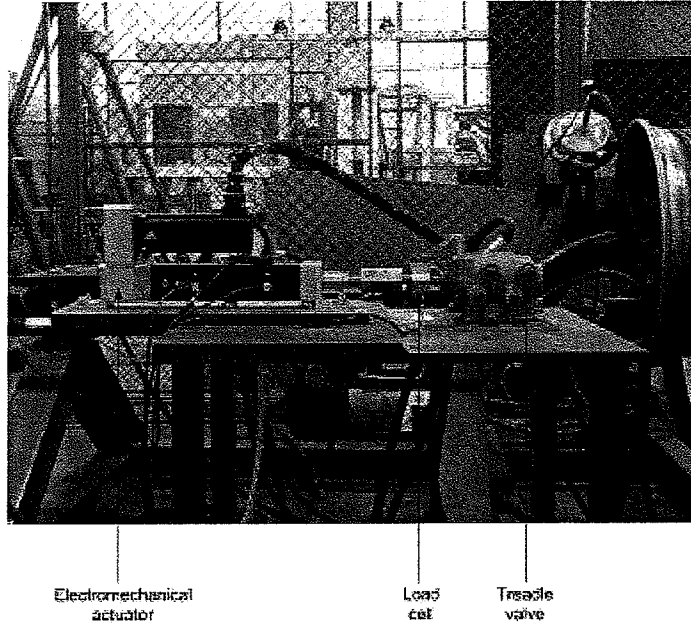


FIGURE 3: Test setup at Texas A&M University.

A closed loop position feedback control system is used to regulate the displacement of the treadle valve plunger. An EC2 electric cylinder (mounted with a B23 brushless servo motor) manufactured by Industrial Devices Corporation/Danaher Motion is used for actuation [4]. The actuator is controlled by a B8501 Servo Drive/Controller [5] [6]. A linear potentiometer is inbuilt in the electric cylinder and its output is provided to the servo drive. The desired plunger motion trajectory is provided from the computer to the servo drive through a Data Acquisition (DAQ) board. The servo controller compares the difference between the desired displacement and the measurement from the linear potentiometer at each instant in time and provides the suitable control input to the actuator. The position control system is tuned to obtain the desired performance using IDC Servo Tuner software program [7].

A pressure transducer is mounted at the entrance of each of the four brake chambers by means of a custom designed and fabricated pitot tube fixture. A displacement transducer is mounted on each of the two front brake chamber push rods through appropriately fabricated fixtures in order to measure the push rod stroke. All the transducers are interfaced with a connector block through shielded cables. The connector block is connected to a PCI-MIO-16E-4 DAQ board [8] (mounted on a PCI slot inside a desktop computer) that collects the data during brake application and release. An application program is used to collect and store the data in the computer.

A graduated Flow Control Valve (FCV) [9] is installed to introduce controlled amounts of leak in the system. Four turns of the adjustable dial completely opened the valve. The FCV was installed between the primary delivery of the treadle valve and the brake chamber as shown in the Fig. 4. Leaks of varying degrees are introduced by turning the dial of the FCV by half-a-turn, one full turn, two full turns etc.

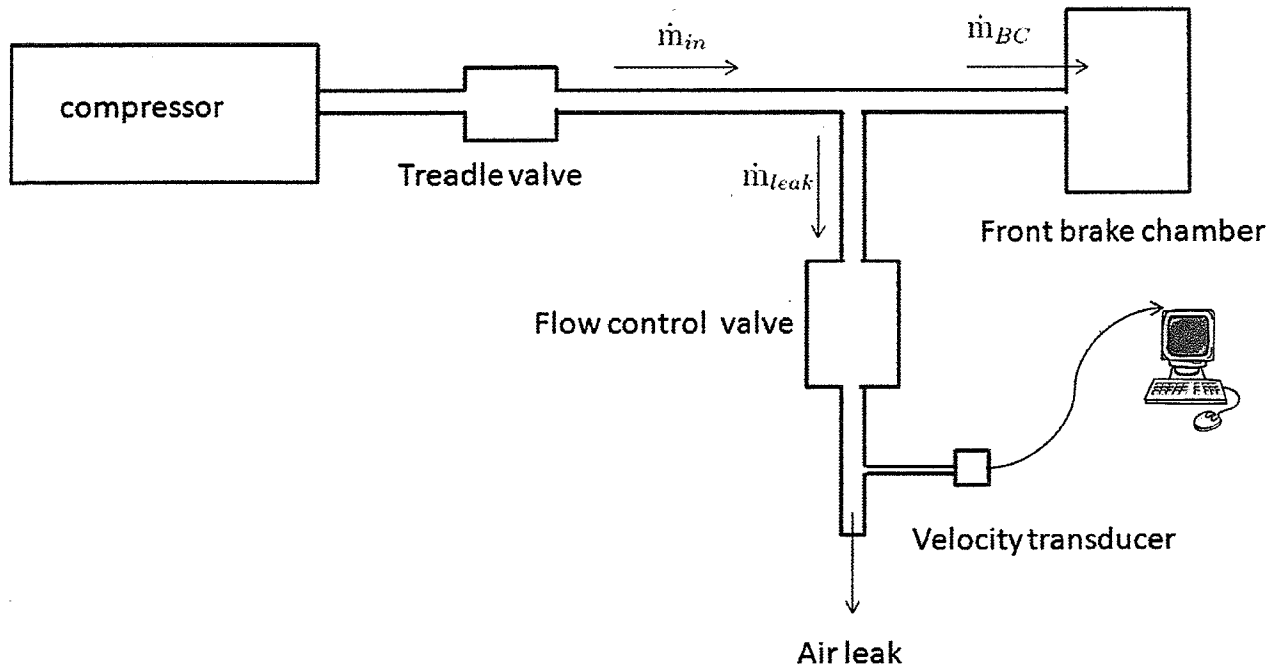


FIGURE 4: Schematic of the leak measurement test setup.

A velocity transducer [10] is installed to measure the mass flow rates of air leaked out of the system. The sensor is interfaced using the DAQ card and the voltage outputs are recorded during the test runs. The voltage outputs from the transducer sensor are then converted to dynamic pressure using the calibration curve of the sensor. This pressure data is then converted to velocity and in turn to mass flow rate. The FCV, velocity transducer and leak measurement setup are shown in Figs. 5, 6 and 7.

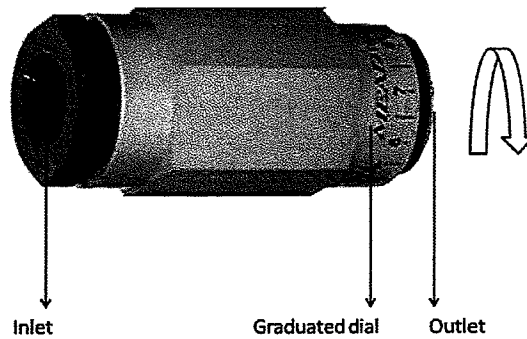


FIGURE 5: Flow Control Valve (FCV).

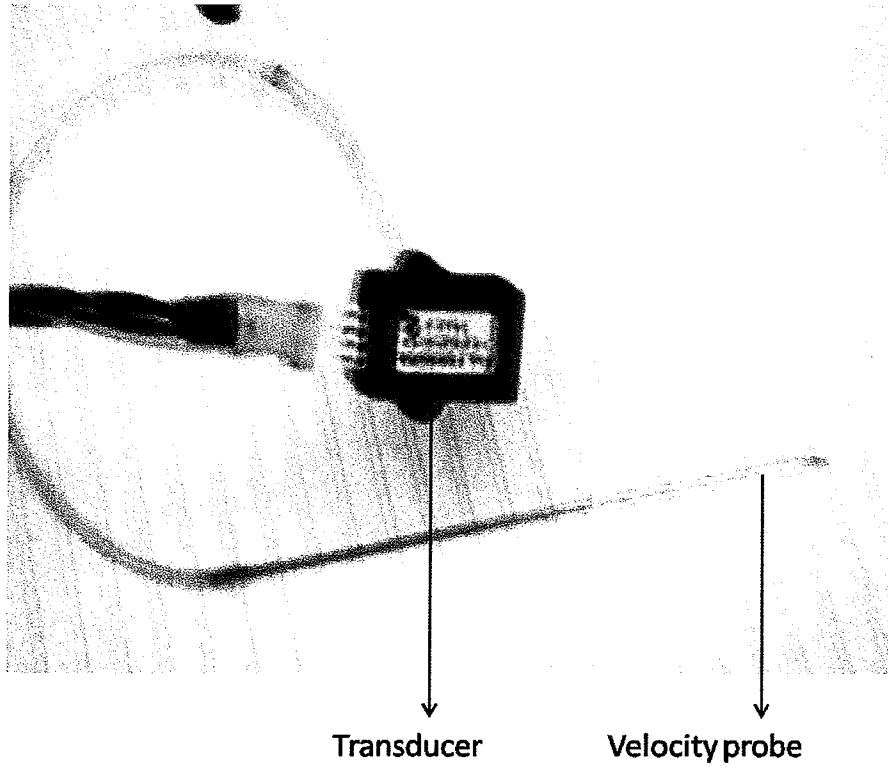


FIGURE 6: Velocity transducer.

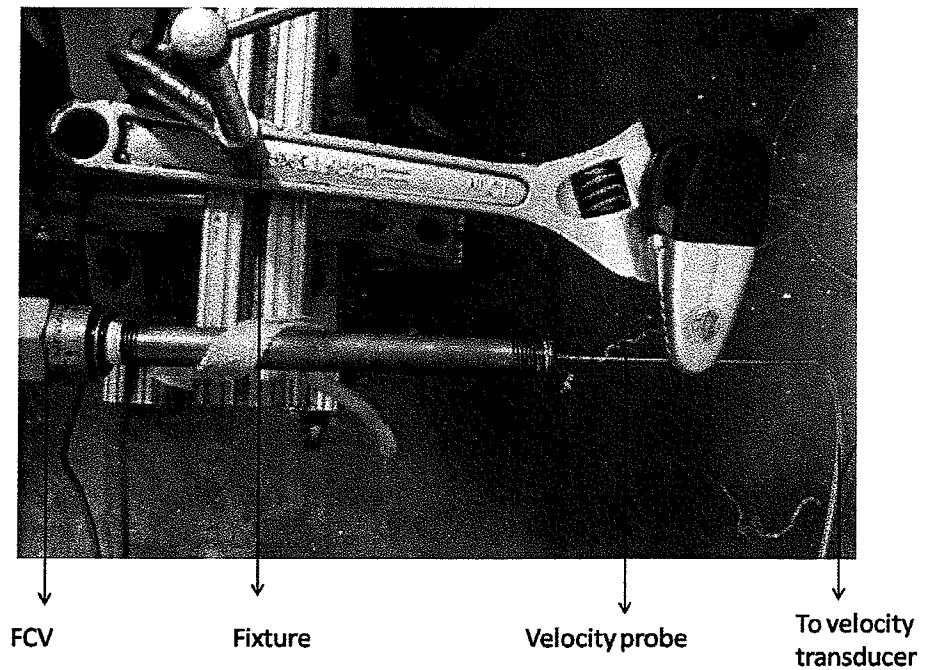


FIGURE 7: Leak measurement setup.

3 Model of the Pneumatic Subsystem

A fault-free model of the pressure transients in a brake chamber of the pneumatic subsystem of the air brake system has been developed by the authors and reported in [11]. In this section we present a summary of the main governing equations of the model. A detailed derivation of the model along with the pertinent assumptions, terminology and nomenclature can be found in [12]. We consider the configuration of the brake system in which the delivery port of the primary circuit is directly connected to one of the two front brake chambers. This configuration is chosen for this first study of developing diagnostic schemes for the air brake system.

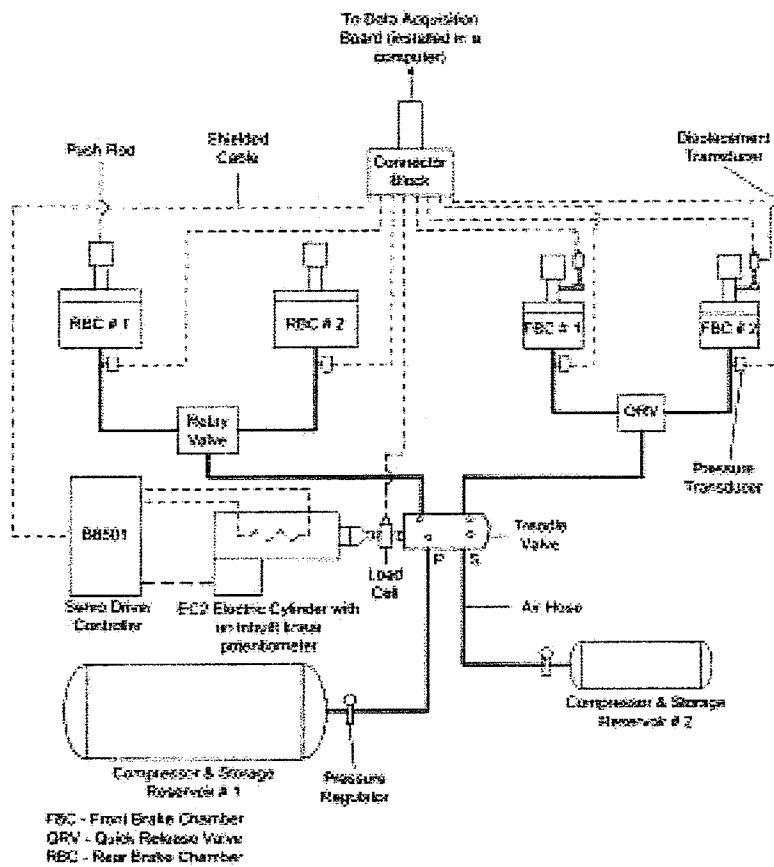


FIGURE 8: Experimental setup.

A cross-sectional view of the brake chamber is presented in Fig. 9. In [12], we assume a single linear relation between the stroke of the push rod and the pressure in the brake chamber till the final stroke is reached.

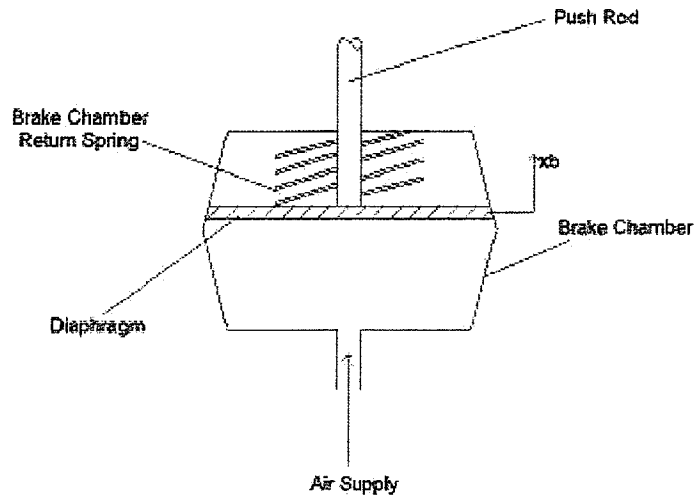


FIGURE 9: Sectional view of the brake chamber.

The brake pad contacts the brake drum at a certain pressure in the brake chamber. Let us call this pressure as contact pressure and denote it by P_{ct} . After this further stroke of the push rod with increasing brake chamber pressure is caused due to the compliance in the mechanical components. Thus the total stroke of the push rod is made up of two components one that is required to overcome the clearance between the brake pad and the brake drum and another that is due to the deformation of the mechanical components after the brake pad makes contact with the brake drum. Thus the total stroke of the push rod depends both on the brake pad-drum clearance and the steady state pressure in the brake chamber. We have included these effects in our model. We have approximated these two regions with linear models and have obtained a calibration curve relating the push rod stroke to the brake chamber pressure.

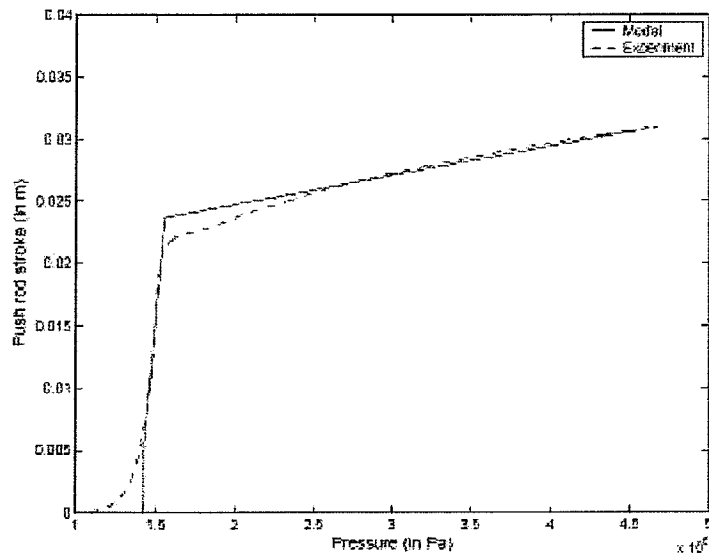


FIGURE 10: Calibration curve at 653kPa (80 psig) supply pressure.

The calibration curve relating the push rod stroke and the brake chamber pressure is shown in Fig. 10. The calibration constants are obtained from this curve and used for all the subsequent test runs. We note that once we fix the threshold pressure (P_{th}), the final push rod stroke can be determined if the parameter P_{ct} and the steady state pressure are known. Thus, the volume of the brake chamber (V_b) is given by (we refer the reader to [12] for a description of the symbols appearing in the following equations) where the constants M_1 , M_2 and N_1 are obtained from the calibration curve shown in Fig. 10. Thus, the governing equations for the operation of the primary circuit during the apply and hold phases [12] of the brake application are given by

$$V_b = \begin{cases} V_{o1} & \text{if } P_b < P_{th} \\ V_{o1} + A_b(M_1 P_b + N_1) & \text{if } P_{th} \leq P_b \leq P_{ct} \\ V_{o1} + A_b(M_2(P_b - P_{ct}) + M_1 P_{ct} + N_1) & \text{if } P_b \geq P_{ct} \end{cases} \quad (1)$$

$$K_2 x_{pp} = K_{ss} x_{pp} + F_{gs} + F_1 - P_{pd}(A_{pp} - A_{pv}) - P_{ps} A_{pv1} + P_{atm} A_{pp} \quad (2)$$

$$x_{pv}(t) = x_{pp}(t) - x_{pt} \quad (3)$$

$$\begin{aligned} & \left(\frac{2\gamma}{(\gamma-1)RT_0} \left[\left(\frac{P_b}{P_o} \right)^{\frac{2}{\gamma}} - \left(\frac{P_b}{P_o} \right)^{\frac{\gamma+1}{\gamma}} \right] \right)^{\frac{1}{2}} A_p C_D P_o \operatorname{sgn}(P_o - P_b) \\ & = \begin{cases} \left(\frac{V_{o1} P_o^{\frac{\gamma-1}{\gamma}}}{\gamma RT_0 P_o^{\frac{\gamma-1}{\gamma}}} \right) \dot{P}_b & \text{if } P_b < P_{th} \\ \left(\frac{V_b P_o^{\frac{\gamma-1}{\gamma}}}{\gamma RT_0 P_o^{\frac{\gamma-1}{\gamma}}} + \frac{P_b^{\frac{1}{\gamma}} A_b M_1 P_o^{\frac{\gamma-1}{\gamma}}}{RT_0} \right) \dot{P}_b & \text{if } P_{th} \leq P_b < P_{ct} \\ \left(\frac{V_b P_o^{\frac{\gamma-1}{\gamma}}}{\gamma RT_0 P_o^{\frac{\gamma-1}{\gamma}}} + \frac{P_b^{\frac{1}{\gamma}} A_b M_1 P_o^{\frac{\gamma-1}{\gamma}}}{RT_0} \right) \dot{P}_b & \text{if } P_b \geq P_{ct} \end{cases} \quad (4) \end{aligned}$$

where during the apply phase

$$A_p = 2\pi r_{pv} x_{pv} \quad (5)$$

We note that when the primary delivery port is directly connected to a front brake chamber, the pressure of air at the primary delivery port (P_{pd} in Eq. (2)) is taken to be the same as the pressure of air in the brake chamber (P_b in Eq. 2). The above equations are solved numerically to obtain the pressure transients in the brake chamber during the apply phase of a brake application cycle. The input to the simulations is the displacement of the treadle valve plunger (x_p). The equations are solved using fourth order Runge-Kutta numerical scheme to obtain the pressure transients. The pressure transients predicted by the model agree very well with experimentally obtained pressure data and is presented in Fig. 11.

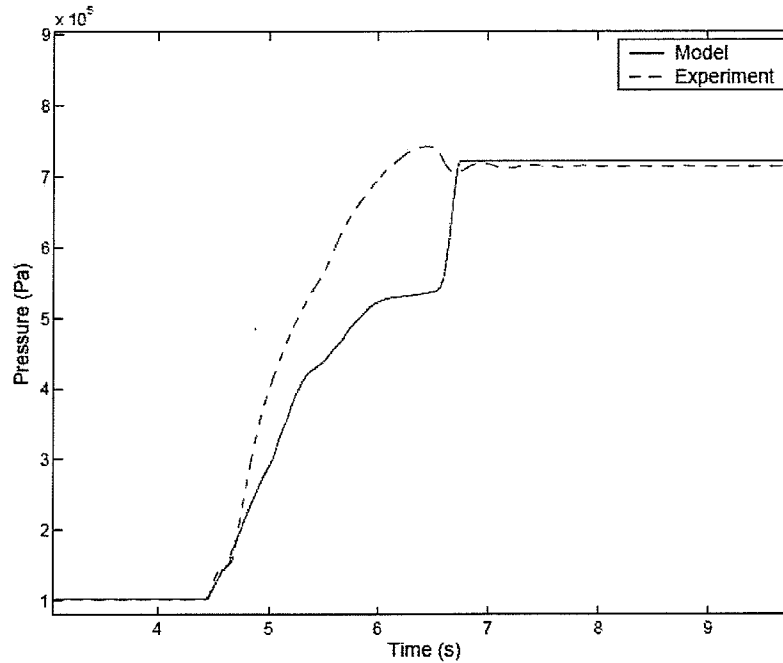


FIGURE 11: Pressure transients at 90psig supply.

Equations (1) to (5) constitute the no-leak or the “fault-free” model of the air brake system, which form the basis of obtaining the pressure transients in the brake chamber in the presence of leaks. This is discussed in the subsequent section.

4 Modeling Pressure transients in the Presence of Leak

The “fault-free” model described above predicted the pressure transients reasonably well if there were no leaks in the system. Modeling the pressure transients in the presence of leaks will help in comparing the rise times for pressure evolution with the norms specified by FMVSS [3]. Estimation of stopping distances from brake torque measurements require the rise time for pressure build up, which can be obtained from such models.

The governing equations are developed for a brake system configuration considered in the “fault-free” model (a front brake chamber directly connected to the primary delivery of the treadle valve). The leak is assumed to be near the brake chamber and after the treadle valve as shown in Fig.4. Site of the leak is assumed to behave like a nozzle. Since air leaks to the atmosphere, and since the ratio of supply pressure to atmospheric pressure is greater than the critical pressure ratio [13], choked flow conditions are assumed. By conservation of mass,

$$\dot{m}_{in} - \dot{m}_{leak} = \dot{m}_{BC} \quad (6)$$

where the total mass flow rate from the treadle valve is denoted by \dot{m}_{in} , the mass flow rate of air leaked to atmosphere is denoted by \dot{m}_{leak} and the mass flow rate of air entering the brake chamber is denoted as \dot{m}_{BC} . The expression for \dot{m}_{in} is the expression on the left hand side of Eq.(4) and the expression for \dot{m}_{BC} for various modes of operation is the expression on the right hand side of Eq. (4).

4.1 DERIVATION OF \dot{m}_{leak}

It was observed from experiments that the mass flow rate of air leaked out increased with increase in supply pressure as well as increase in area of the leak (determined by the no. of turns of FCV). This is shown in Fig.12.

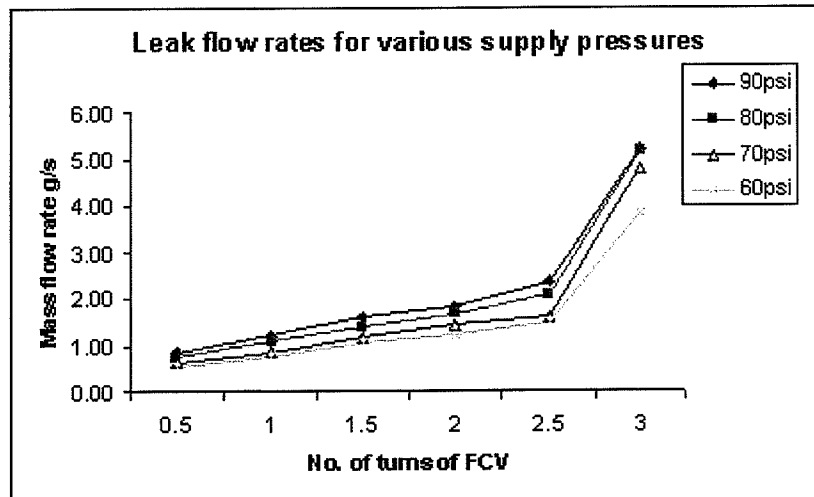


FIGURE 12: Leak flow rates at various supply pressures and FCV settings.

Hence \dot{m}_{leak} may be assumed to be of the form,

$$\dot{m}_{leak} = f(P_{sup}, A_l) \quad (7)$$

where P_{sup} is the supply pressure and A_l is the area of leak. In reality, area of the leak, A_l , may not be known a priori. Yet it has to be incorporated into the model as it is one of the input variables along with supply pressure, P_{sup} . We will assume the following constitutive relationship for the mass flow rate of leaking air:

$$\dot{m}_{leak} = C_d A_l \frac{P_{sup}}{\sqrt{RT}} \sqrt{\left(\frac{2}{\gamma+1}\right)^{\frac{\gamma+1}{\gamma-1}}} \quad (8)$$

where C_d is the coefficient of discharge, γ is the ratio of specific heats for air, R is the universal gas constant for air. We will define K as:

$$K = \frac{C_d A_l}{\sqrt{R}} \sqrt{\left(\frac{2}{\gamma+1}\right)^{\frac{\gamma+1}{\gamma-1}}} \quad (9)$$

so that

$$\dot{m}_{leak} = \frac{K P_{sup}}{\sqrt{T}} \quad (10)$$

The term $C_d A_l$ will be referred as “effective leak area” since the actual leak area is not known. Once the effective area of leak is determined, it is input to the leak expressions in Eq. (8) and Eq. (6) to obtain the desired mathematical model.

4.2 ESTIMATION OF EFFECTIVE LEAK AREA

We will use a least squares approach to determine the area of the leak [14]. Since we can measure the mass flow rate of leaking air, the supply pressure and the temperature (of air leaking out), we can determine the value of K that minimizes the least squares error given below:

$$err = \sum_{i=1}^N (\dot{m}_{meas}^{(i)} - K \frac{P_{sup}^{(i)}}{\sqrt{T}})^2 \quad (11)$$

where, N is the total number of samples, i is the sample number, $\dot{m}_{meas}^{(i)}$ is the measured leak mass flow rate. Parameter K was found for leak measurements performed at different supply pressures (90 psi, 80 psi etc) and at different FCV settings (half-a turn, single turn etc) .The corresponding effective leak area, $C_d A_l$ is then immediately obtained from Eq.(9).

4.3 EXPERIMENTAL PROCEDURE

Several leak measurements were performed to collect the mass flow rates of leak during a full brake application. For a given supply pressure, say 90 psi, leaks were introduced in the system in steps of half-a-turn until two-and-a-half turns of the FCV. This was repeated for other supply pressures say 80 psig, 70 psig etc.

4.3.1 Corroboration of Measurements

A series of experiments were conducted to corroborate the leak flow measurements prior to the actual leak measurements in the brake system. The compressor delivery was directly connected to the FCV. For each leak setting, the compressor was allowed to drain completely. Since the DAQ card could collect data continuously for only 60 seconds [8], the experiments were conducted as follows.

Compressor was allowed to drain for 60 seconds at a particular FCV setting. FCV was closed at the end of 60 seconds. Steady state compressor delivery pressure was noted at the start and also at the end of the 60 second interval. Data was collected from the velocity transducer continuously for the 60 second period. This was repeated at the same FCV setting till all the air in the reservoir was drained out. A schematic of the setup is given in Fig. 13.

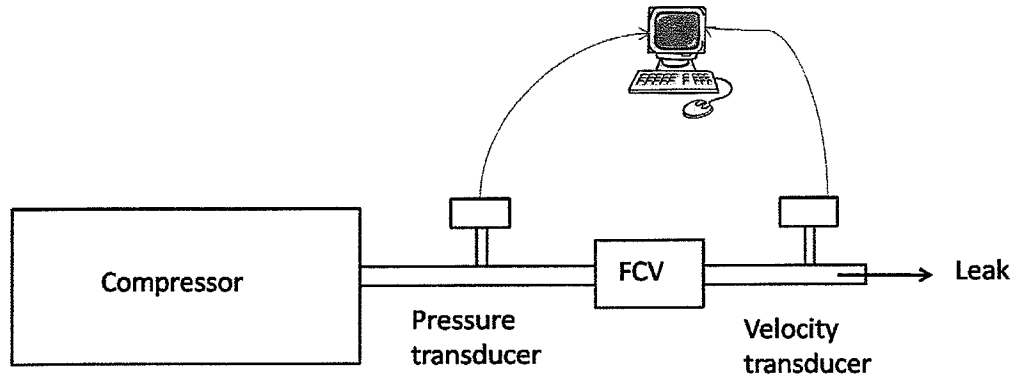


FIGURE 13: Schematic of the setup for leak corroboration tests.

Since the leak flow is very turbulent, average velocity of flow was computed from the measured velocity using the “one-seventh” power law approximation of velocity profiles [15]. The ratio of average velocity to the measured centerline velocity was found to be

$$\frac{\bar{V}}{U} = \frac{2n^2}{(n+1)(2n+1)} \quad (12)$$

where, \bar{V} is the average velocity, U is the measured centerline velocity, n is a constant and is equal to 7. The average velocity \bar{V} is utilized for all the mass flow rate calculations. From the mass flow rates calculated using Eq. (11), the total amount of air leaked from the compressor was found by integrating the mass flow rates with respect to time. This was compared with the values predicted by the ideal gas equation. Multiple runs were conducted to test for repeatability

of measurements. The measured values were found to be in close agreement. Comparison of one such run performed at two turns of FCV is presented in Fig.14.

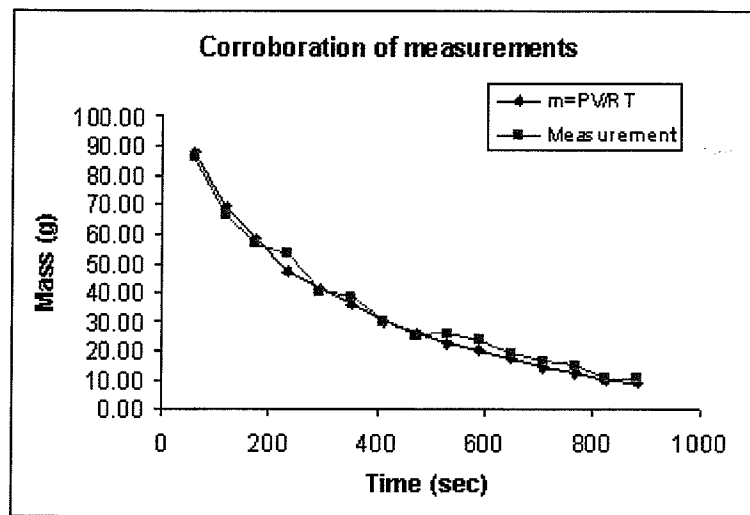


FIGURE 14: Comparison of measured and predicted mass values at two turns of FCV.

4.3.2 Leak measurements

Once the measurements were corroborated, the desired leak measurement experiments were performed using the setup described in Fig 4. The measured leak mass flow rates are tabulated in Table and Table 2.

Table 1 Leak mass flow rates for a full brake application at 90 psi supply pressure

Supply pressure (psi)	No. of turns of FCV	Mass flow rate (g/s)
90	0.5	0.83
	1	1.18
	1.5	1.6
	2	1.82
	2.5	2.35
	3	5.21

Table 2 Leak mass flow rates for a full brake application at 80 psi supply pressure

Supply pressure (psi)	No. of turns of FCV	Mass flow rate (g/s)
80	0.5	0.74
	1	1.10
	1.5	1.4
	2	1.66
	2.5	2.06
	3	5.18

It can be easily inferred from Fig.12, that there is a sudden jump in the mass flow rates of air leaked out between 2.5 turns and 3 turns of the FCV. Leaks greater than three turns of the FCV resulted in very small pressure build up in the brake chamber. Such large leaks were not considered since warning devices for such occurrences are already in place. Moreover, the schemes we are developing for small leaks are expected to provide warnings well in advance that one would not be in such a situation. Therefore, only “small leaks” (up to 2.5 turns of FCV) were taken into consideration. Thus, these mass flow rates were input into the leak flow models to estimate K , C_dA_l and the pressure transients were obtained in the presence of leak. Since FMVSS norms [3] dictate that all leak tests be done at full brake application and at a reservoir pressure of 90 psi, results for this supply pressure will be presented and discussed in detail in the subsequent sections.

4.4 CORROBORATION OF THE MATHEMATICAL MODEL IN THE PRESENCE OF LEAK

From the leak mass flow rates, the parameter K and C_dA_l are estimated and presented in Table 3. A key point to be noted is that C_dA_l doesn't represent the actual area of the leak i.e., the opening of the FCV. It is an “effective” area of leak. An effective area of $4.8e-6 \text{ m}^2$ may be visualized as an equivalent circular aperture of a diameter of 2.5mm [14]. The effective areas of leak for corresponding FCV settings are then input into the leak flow model and the governing equations.

Table 3 Estimates of K and effective leak area

Supply pressure (psi)	No. of turns of FCV	K	$C_dA_l \text{ m}^2$
90	0.5	1.940E-07	4.832E-06
	1	3.229E-07	8.045E-06
	1.5	4.779E-07	1.191E-05
	2	5.778E-07	1.440E-05
	2.5	7.646E-07	1.905E-05

The results of the simulations are compared with experimentally obtained measurements and are presented in Fig.15 and Fig.18. The comparison between the predicted and the measured values is presented in Table 4.

Table 4 Comparison of model and measured steady state pressures

Supply pressure (psi)	No. of turns of FCV	P_{meas} (psi)	P_{model} (psi)	Error %
90	0.5	87.28	89.58	-2.72
	1	86.76	89.00	-2.58
	2	85.78	86.53	-0.88
	2.5	85.53	84.07	1.71

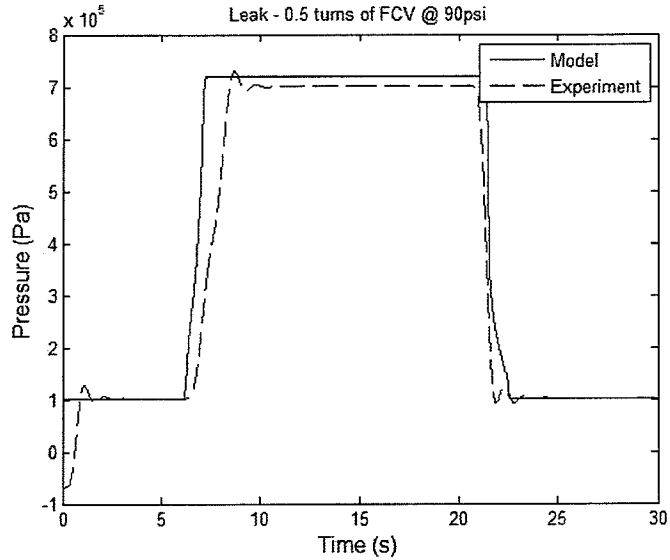


FIGURE 15: Pressure transients at 90 psi supply and 0.5 turns of FCV.

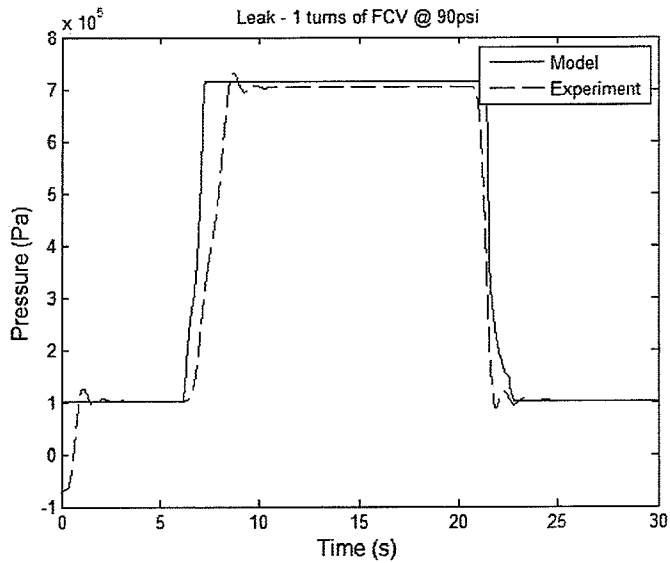


FIGURE 16: Pressure transients at 90 psi supply and 1 turn of FCV.

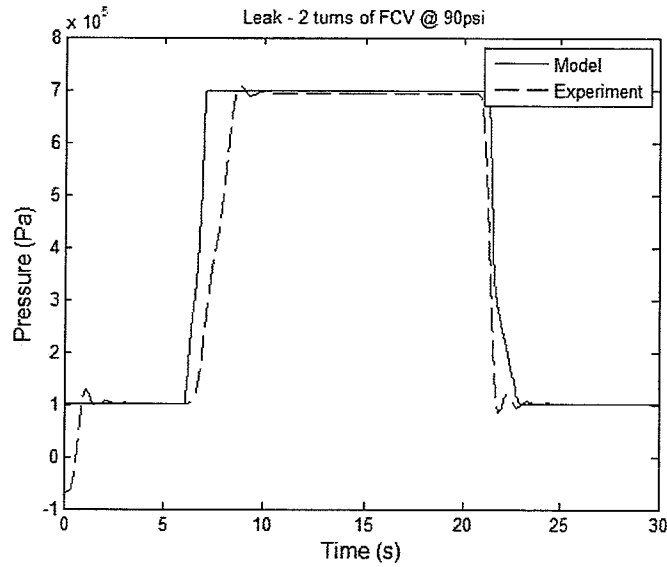


FIGURE 17: Pressure transients at 90 psi supply and 2 turns of FCV.

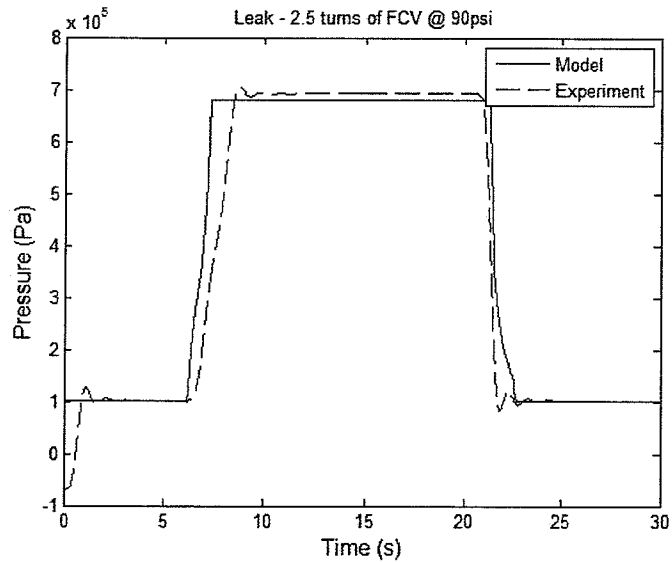


FIGURE 18: Pressure transients at 90 psi supply and 2.5 turns of FCV.

It can be seen that the model predicts the pressure transients in the presence of leaks reasonably well. P_{meas} is the experimentally measured steady state pressure. P_{model} is the steady state brake chamber pressure predicted by the model. Percentage error is defined as $(P_{meas} - P_{model}) \times 100 / P_{meas}$. The model over predicts the experiment in the first two cases and under predicts for the last case. The model matches very closely the experimental results for FCV setting of 2 turns.

4.5 “REALISTIC LEAKS”

To simulate realistic leaks, a set of flow control orifices [16] were installed instead of the FCV to introduce leaks. The orifices ranged from 0.4mm diameter to 1.6mm diameters. Experiments were run at full brake application with leak introduced through these orifices. In the case of real time leaks, the only diagnostic data available would be the measured steady state brake chamber pressure. Based on this value, one must be able to make a judgment whether there is leak in the system or not.

This can be done by comparing the steady state pressure attained during a test with the values obtained in Tables 1 and 4. For example, let the measured steady state pressure during a full brake application with 90 psi supply be 83 psi. Looking up Table 4, it can be inferred that a leak is present whose magnitude is slightly greater than 2.5 turns of FCV (effective area 19mm²). To quantify it precisely, from Table.1, we can conclude that the severity of the leak is given by a leak flow rate greater than 2.35 g/s. Hence Tables 1 to 4 serve as a “master look-up” data for leaks. From the leak model, the measured steady state pressure is used to obtain the effective area of leak using the calibration curve (obtained by plotting the steady state pressure values predicted by the model in Table.4 with the effective areas obtained from Table.3),

$$C_d A_l = -2.4945 P_{ss} + 229.34 \quad (13)$$

where, $C_d A_l$ is in mm², P_{ss} is the measured steady state pressure in psi. The $C_d A_l$ hence obtained is input to the leak model to predict the pressure transients due to leak caused by orifices. The results are summarized in Table 5 and a comparison is shown for one particular orifice data in Fig 19.

Table 5 Estimates of K and effective leak area for the orifices

Supply Pressure (psi)	Orifice dia (mm)	Steady state pressure (psi)	K	$C_d A_l$ mm ²
90	0.5	87.34	5.189E-08	11.47
	1	86.53	2.192E-07	13.48
	1.2	86.51	3.002E-07	13.55
	1.4	85.86	4.192E-07	15.16
	1.63	82.53	5.694E-07	23.46

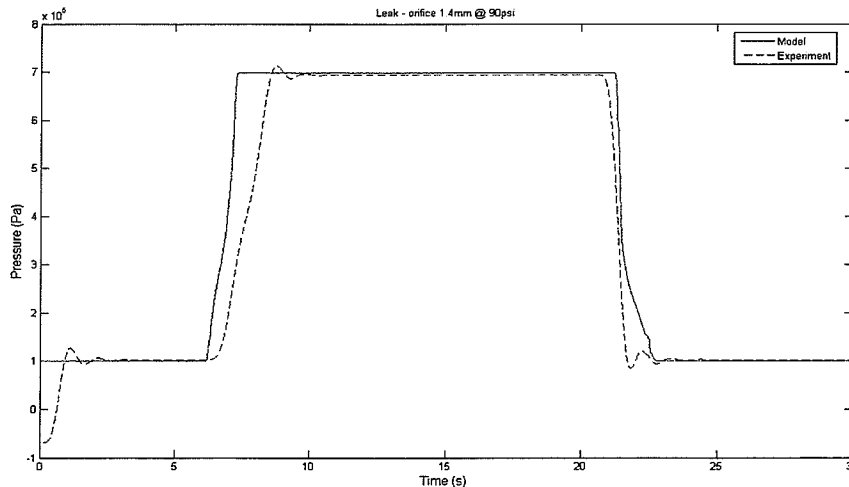


FIGURE 19: Pressure transients at 90 psi supply with 1.4mm orifice.

5 Push rod stroke estimation

In this section, two schemes for estimating the stroke of the push rod from the measurement of the brake chamber pressure are discussed. The final stroke of the push rod is made up of two parts – the first part is for overcoming the clearance between the brake pads (Mode 2) and the brake drum. The second part is due to the subsequent deformation of the mechanical components (Mode 3) till the steady state pressure is achieved. The steady state stroke of the push rod (x_{bss}) can be written as

$$x_{bss} = M2(Pb_{ss} - Pct) + M1Pct + N1 \quad (14)$$

where Pb_{ss} is the steady state brake chamber pressure. The value of Pb_{ss} can be found from the measured pressure data. Thus, the problem of estimating the final stroke is equivalent to obtaining a good estimate of the parameter Pct (which is the brake chamber pressure at which the clearance between the brake pads and the brake drum is overcome). Two schemes are now presented that provide an estimate of Pct and thus an estimate for the push rod stroke. In the first scheme, the range of possible values of Pct is discretized into sufficiently small intervals. Then, a pressure residue measure is calculated for each possible value of Pct and the one that minimizes this measure is taken to be the estimate of Pct . In the second scheme, a method is proposed for detecting the transition from Mode 2 to Mode 3 and subsequently an estimate of Pct is obtained.

5.1 ESTIMATION OF THE PUSH ROD STROKE BY DISCRETIZATION OF THE POSSIBLE RANGE OF VALUES:

In this scheme, the following procedure is proposed to obtain an estimate of Pct :

- 1) From the physical limits on the stroke of the push rod, bounds on the value of Pct can be obtained. Let $Pctl$ and $Pctu$ denote respectively the lower bound and the upper bound on Pct . It should be noted that the lower bound corresponds to zero clearance between the brake pad and the brake drum and the upper bound is obtained from the maximum possible push rod stroke. The maximum push rod stroke for the “Type-20” brake chamber that is being used in the experimental setup is 0.05715 m (2.25 in). The value of $Pctl$ is found from experiments to be 142.73 kPa (6 psig) and the value of $Pctu$ is calculated to be 184.1 kPa (12 psig).
- 2) The estimate of Pct , denoted by \hat{P}_{ct} , will lie in the interval between $Pctl$ and $Pctu$. In order to obtain this value, the interval $[Pctl, Pctu]$ is discretized into finer intervals by using a step size (δP) of 689.5 Pa (0.1 psi). Thus, a set P is obtained whose elements are equally spaced by a step size of δP and whose first and last elements are $Pctl$ and $Pctu$ respectively. It was illustrated previously that, the push rod stroke needed to overcome the clearance between the brake pads and the brake drum is reflected in the second region (Mode 2) of the pressure growth curve. Hence, the focus is restricted to this region for obtaining \hat{P}_{ct} .

- 3) Next, the governing equations of the model (Eq. (4)) are solved numerically for each element in the set P to obtain the corresponding solution of the brake chamber pressure. Then, the following pressure error / residue measure is calculated:

$$e_P(P_{cti}) = \sum_{j=0}^k |P_{meas}(j) - P_b(P_{cti})(j)| \quad (15)$$

where $P_{meas}(j)$ is the measured brake chamber pressure at the j th instant of time and $P_b(P_{cti})(j)$ is the solution of the model (at the same instant of time) corresponding to P_{cti} which is given by

$$P_{cti} = P_{ctl} + (\delta P)_i, \quad i = 0, \dots, N, \quad (16)$$

where $\delta P = \frac{(P_{cti} - P_{ctl})}{N}$

- 4) The choice of k in Eq. (15) is determined by the maximum possible dwell time of the system in Mode 2. Depending on the brake pad to brake drum clearance this time interval will vary. But it has been observed from experiments that this time interval is usually not more than 0.3–0.35 seconds. The sampling time used in the experiments is 2 milliseconds. Hence, the value of k is chosen to be 200 (which correspond to a time interval of 0.4 seconds). It should be pointed out that $j = 0$ corresponds to the time instant at which Mode 2 starts. Hence, one starts at the beginning of Mode 2 (which occurs when the brake chamber pressure reaches the threshold pressure (P_{th})) and calculates the quantity $\hat{e}_P(P_{cti})$ given by Eq. (15). This procedure is repeated for each value of P_{cti} and finally an array of values representing the residue measure given by Eq. (15) is generated.

Then, the estimate \hat{P}_{ct} is obtained as

$$\hat{P}_{ct} = \arg \min_{P_{cti} \in \rho} e_P(P_{cti}) \quad (17)$$

The results obtained by using this scheme on two test runs are illustrated in Fig. (20) and Fig (21). Obtaining accurate measurements of the brake chamber pressure and the treadle valve plunger displacement is critical to the successful implementation of this scheme. A digital filter with a cut-off frequency of 1 Hz and 10 Hz. is used to minimize the effect of noise.

In Fig.20, the results obtained for a test run made at 653 kPa (80 psig) supply pressure are plotted. The array of the pressure error / residue is calculated and the minimum value is located and the estimate \hat{P}_{ct} is obtained from P as the value corresponding to this minimum residue. On the ordinate the term “Normalized pressure residue” has been plotted. The values corresponding to this term are obtained by dividing the array of the residues by its minimum value (thus the minimum residue will always be given a value of 1). Once the value of \hat{P}_{ct} is determined an estimate of the final push rod stroke is obtained by using Eq. (14). In this case, the best estimate of the push rod stroke is obtained to be 0.03381 m (1.3311 in) while the measured value of the stroke is 0.03114 m (1.2262 in). It can be observed that the normalized pressure residue corresponding to the actual stroke is around 1.007 which differs by 0.7 % from the residue

corresponding to the estimated stroke. In Fig. 20, the results obtained from a test run performed at a supply pressure of 722 kPa (90 psig) on a different day from the above test run are presented. It is observed that the estimated push rod stroke in this case is 0.03684 m (1.4506 in) while the measured stroke is 0.03181 m (1.2525 in). It can be noted that the normalized pressure residue corresponding to the actual stroke is around 1.009, i.e., a difference of 0.9 % from the minimum value.

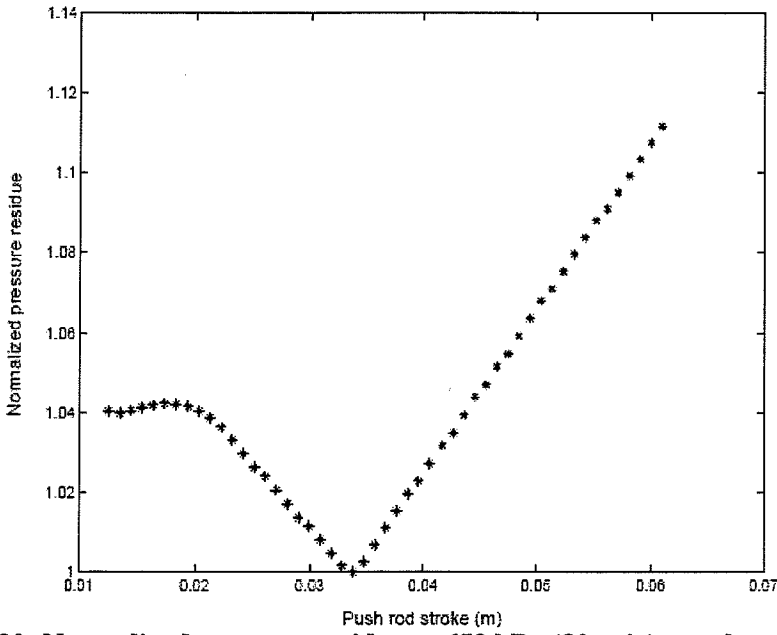


FIGURE 20: Normalized pressure residue at 653 kPa (80 psig) supply pressure

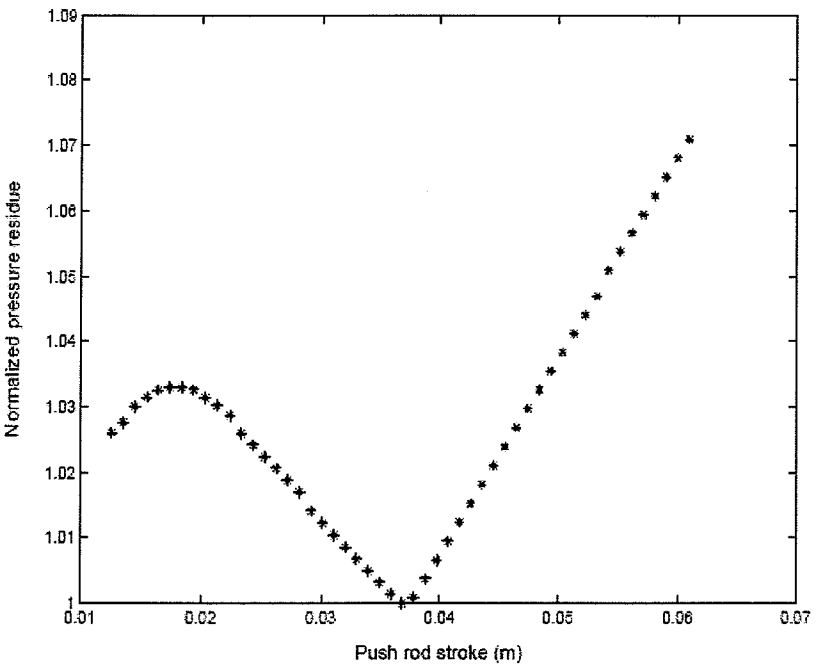


FIGURE 21: Normalized pressure residue at 722 kPa (90 psig) supply pressure

5.2 SCHEME 2 – DETECTION OF THE TRANSITION FROM MODE 2 TO MODE 3

The scheme utilizes the sequential nature of the response of the pneumatic subsystem of the air brake system for detecting the transition from Mode 2 to Mode 3. An estimate of the push rod stroke can be obtained once this transition is detected. The term “transition detection” used here refers to the process of identifying the interval of time during which the system switches from Mode 2 to Mode 3. For the purpose of detecting this transition, a time interval that is smaller than the minimum possible dwell time of the system in Mode 2 is considered. Since the measurements are acquired at a constant sampling time of 2 milliseconds, time intervals shall be represented in terms of the equivalent number of samples in this section.

The following steps are involved in this scheme:

- 1) Let $T1$ denote the instant of time at which the transition occurs from Mode 1 to Mode 2. Since the focus is restricted to only Mode 2 and Mode 3, the data collected at this instant of time is represented by the sample number of 1 for convenience. In the first iteration, the estimate of Pct is taken to be equal to Pth and the governing equations for Modes 2 and 3 are solved numerically over the next K time steps. The value of K is chosen such that it is less than the minimum number of time steps that the system will spend in Mode 2. This can be obtained from experiments and in this case K has been chosen to be 5.
- 2) It is noted that the initial value of the pressure in Mode 3 will be Pct . The input to the numerical scheme is the treadle valve plunger displacement over the time interval corresponding to these K time steps. The governing equations in both modes are solved over K time steps and then the following residue measures are calculated:

$$e_2 = \sum_{j=0}^k |P_{meas}(j) - P_{b2}(P_{cti})(j)|, \quad (18)$$

$$e_3 = \sum_{j=0}^k |P_{meas}(j) - P_{b3}(P_{cti})(j)|, \quad (19)$$

where $Pb2(j)$ and $Pb3(j)$ are the solutions of the governing equations in Mode 2 and Mode 3 respectively.

- 3) If $e_2 < e_3$, it can be concluded that the system is still in Mode 2. The value of Pct is updated to be equal to $P_{b2}(K)$ and the previous step is repeated over the next K time steps.
- 4) If $e_2 \geq e_3$, it can be declared that a transition has taken place from Mode 2 to Mode 3.
- 5) Then, the best estimate of Pct will be the value used at the start of this particular iteration. Once this is known, an estimate of the push rod stroke can be obtained from Eq. (14). In Fig. 22 and Fig.23, the results of this scheme are illustrated on the two test runs that have been considered. The initial time interval is taken to be that corresponding to 50 time steps. This was picked on practical considerations since it is known that the clearance between the brake pads and the brake drum is never zero and usually a minimum stroke

of around 0.0127 m (0.5 in) is needed to overcome this clearance. Such a choice also ensures that any initial disagreement between the model and the experiment at the end of Mode 1 will not affect the transition detection process. Additionally, it reduces the computation time involved.

In Table 6, a comparison of the push rod stroke estimate obtained from these two schemes with the measured stroke is presented. It should be pointed out that the computation time involved in implementing Scheme 2 is much less than that of Scheme 1 and this would be beneficial for implementing the diagnostic scheme in practice. Also, the complexity of Scheme 1 will increase if more than one unknown parameter needs to be estimated. For example, if the value of P_{th} were unknown in addition to that of P_{ct} , one needs to obtain the pressure residue measure for each possible pair of values of P_{th} and P_{ct} using Scheme 1. But, using Scheme 2, an estimate of P_{th} can be obtained by detecting the transition from Mode 1 to Mode 2.

Thus, a reasonable estimate of the push rod stroke can be obtained by using these two schemes. Although it is difficult to pin-point a particular value of the push rod stroke as the best estimate (due to the experimental issues discussed above), one can provide a range of values for the best estimate depending on a chosen range for the tolerated normalized pressure residue. For example, using Scheme 1, one can identify the region of the push rod stroke estimate as that corresponding to the interval [1, 1.01] for the normalized pressure residue (i.e., till 1 % more than the minimum). A range of possible estimates of the actual push rod stroke is practically valuable since one can determine the state of the push rod adjustment from it.

5.3 RESULTS AT 90 psi SUPPLY UNDER NO LEAK CONDITIONS

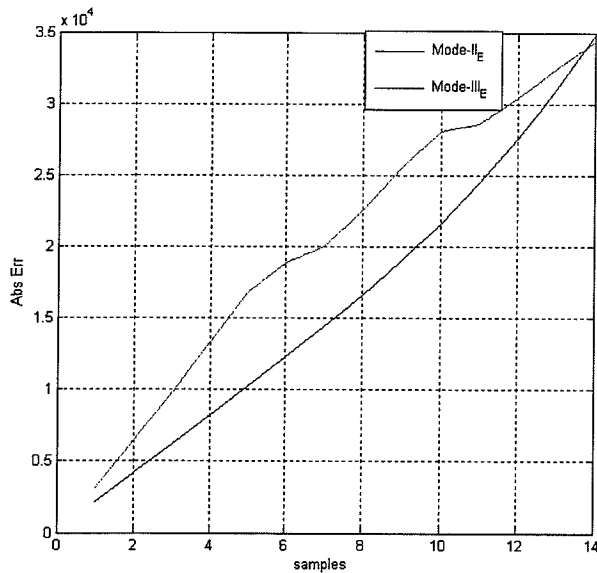


FIGURE 22: Error Mode-II & III Pct=1.52 bar

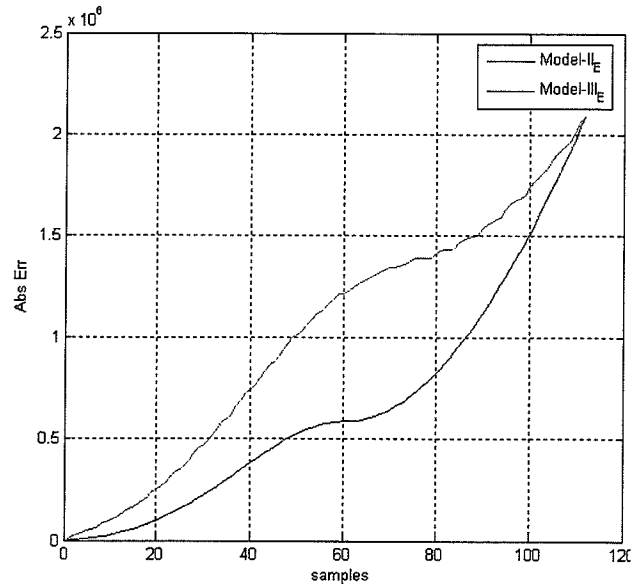


FIGURE 23 Error Mode -II & III Pct = 1.57 bar

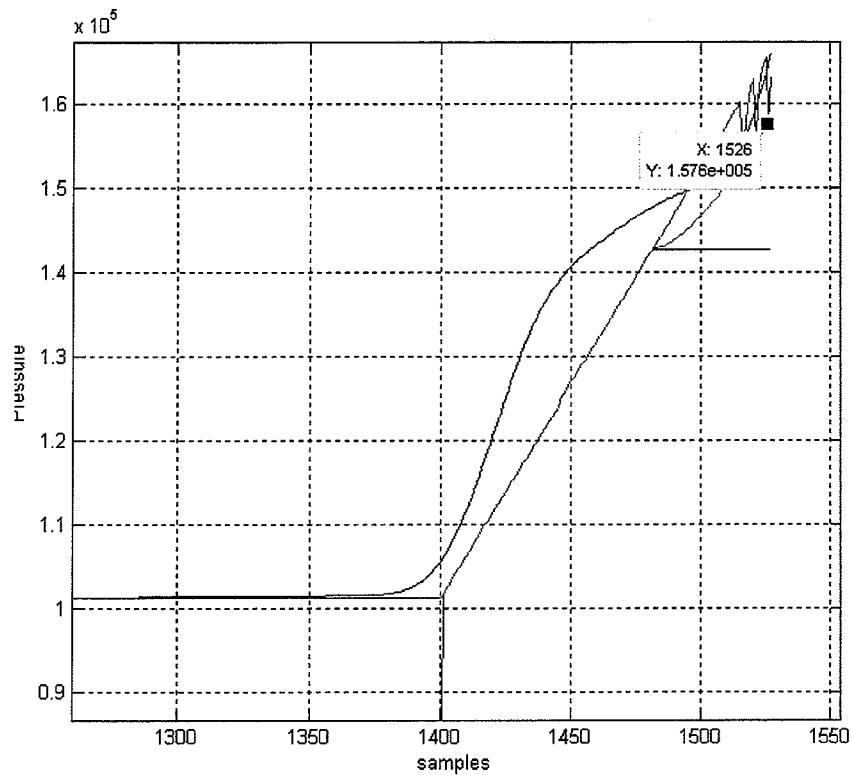


FIGURE 24: Transition detection at 722 kPa (90 psig) supply pressure

Table 6 Comparison of the Actual and the Estimated Push Rod Stroke

Supply pressure kPa / psig	Actual stroke (m/in)	Scheme 1 (m / in)	Scheme 2 (m / in)
653 / 80	0.03114/1.2262	0.03381/1.3311	0.03526/1.3883
722 / 90	0.03181/1.2525	0.03684/1.4506	0.03755/1.4784

5.4 PUSH ROD STROKE ESTIMATION IN THE PRESENCE OF A LEAK

The estimation of push-rod stroke in the presence of a leak involved a modified form of scheme 2. The modification is the incorporation of the leak model (discussed in section 4) into the mode 2 and mode 3 equations (Eq. 6). The computed push rod stroke using the modified scheme 2 was reasonably close to the experimentally obtained push rod stroke measurements. Based on experimental data, it is observed that with the leak introduced in the system, the steady state push rod stroke is lower than the steady state stroke attained under no leak conditions. The modified scheme 2 correctly predicted the decrease in the push rod stroke. The results of the estimation scheme are presented from Fig.25 to Fig.28 and in Table 7.

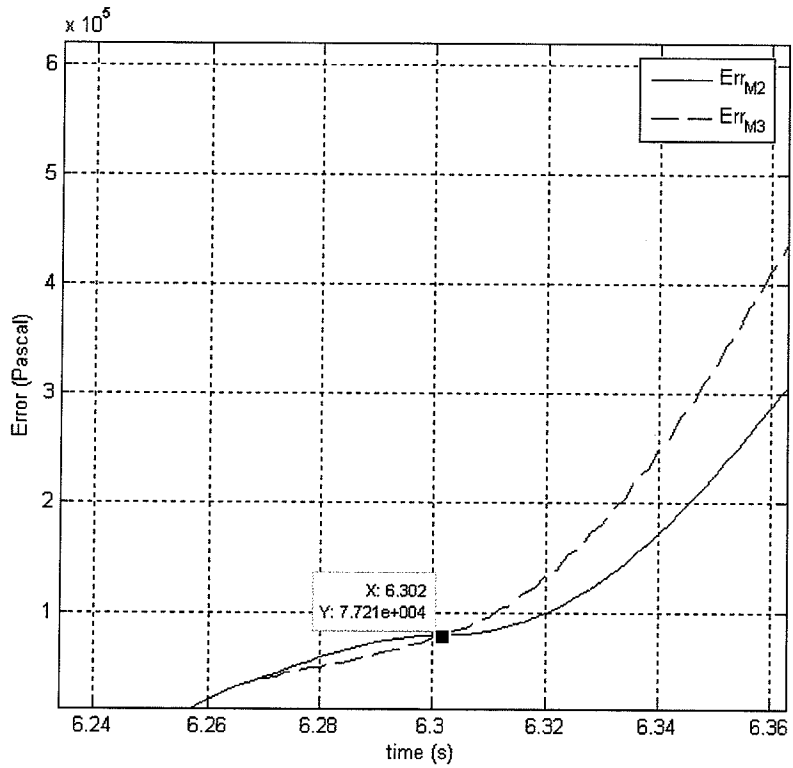


FIGURE 25: Error in Mode-II & III for 90 psig supply (FCV ¼ open)

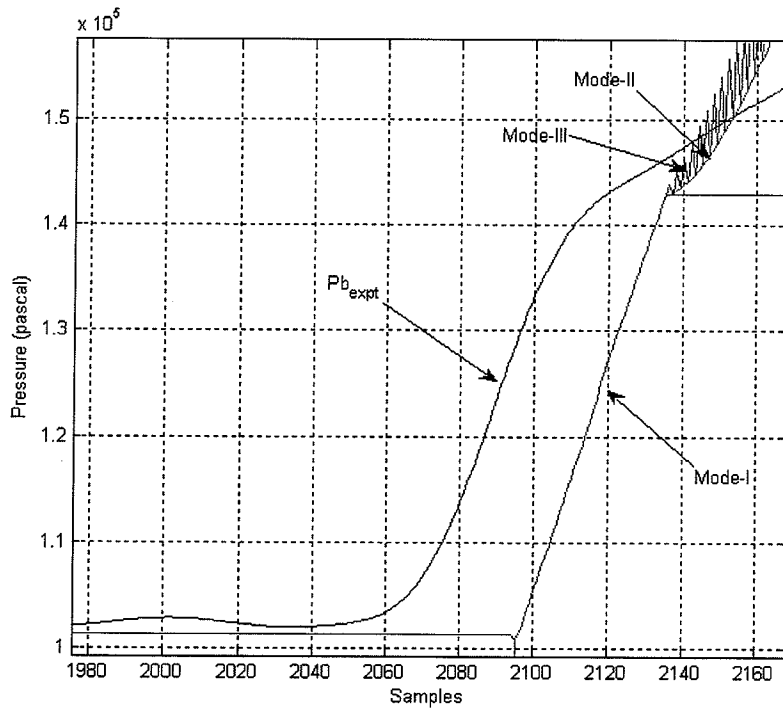


FIGURE 26: Transition detection at 722 kPa (90 psig) supply pressure (FCV ¼ open)

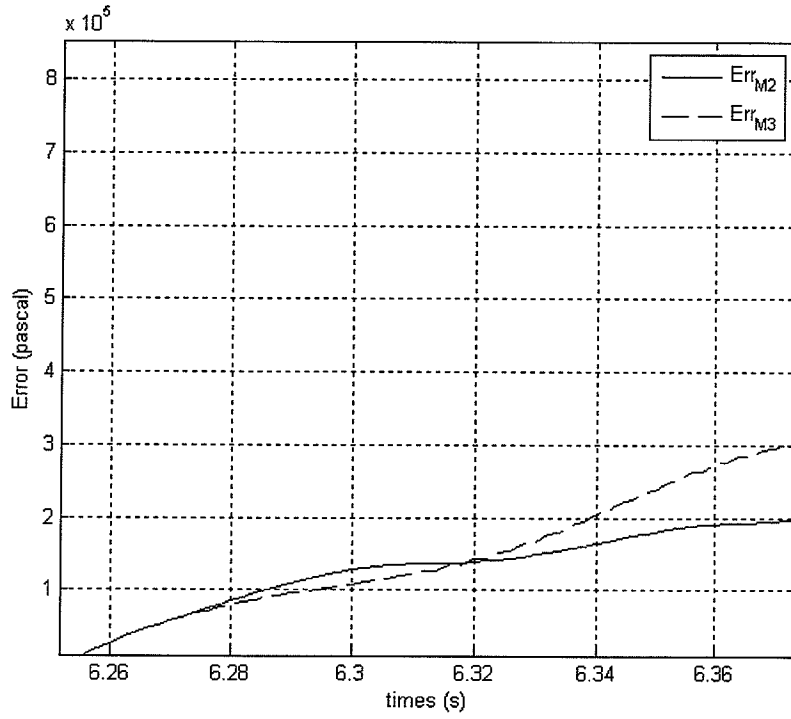


FIGURE 27: Error in Mode-II & III for 80 psig supply (FCV ¼ open)

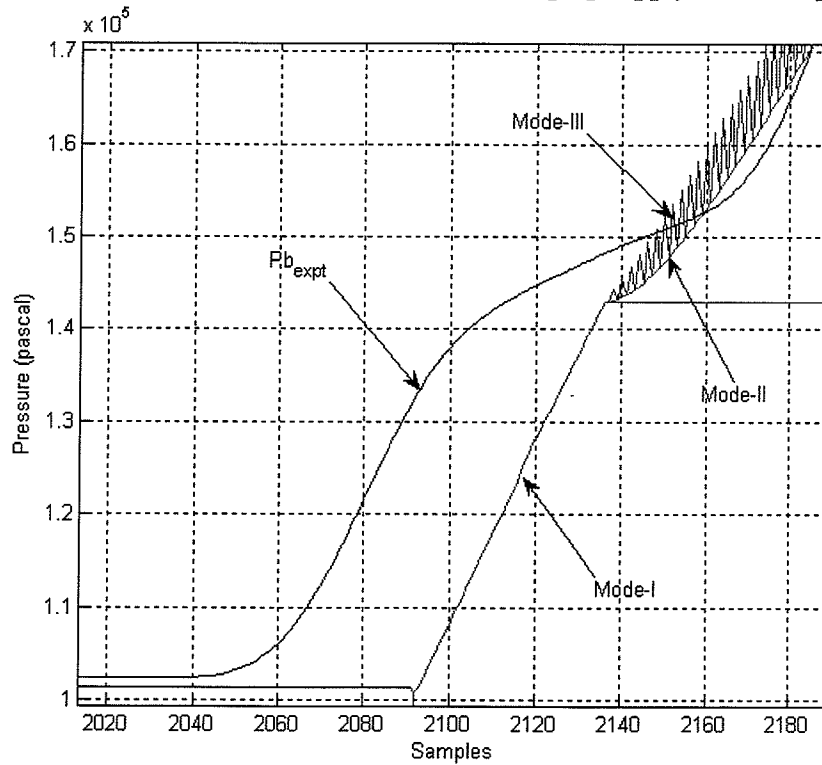


FIGURE 28: Transition detection at 722 kPa (90 psig) supply pressure (FCV ¼ open)

Table 7 Comparison of the Actual and the Estimated Push Rod Stroke (with leak)

Supply Pressure kPa / psig FCV ¼ open	Actual stroke (m / in)	Scheme 2 (m / in)
653 / 80	0.0319278 / 1.257	0.03111426 / 1.225
722 / 90	0.0335026 / 1.319	0.028745 / 1.1317

6 Conclusions

The purpose of this project was to enhance the safety of trucks by developing diagnostic systems that assess the health of a brake system. This project consisted of three stages – the first one dealt with the development of a leak detection algorithm in the absence of a leak, the second one dealt with the development of a pushrod stroke estimation algorithm in the absence of a leak and the third stage dealt with the development, experimental implementation, testing and evaluation of a prototype system incorporating these algorithms when there is a leak. The presence of leaks necessitated the development of algorithms that estimated the “severity” of leaks as well as algorithms that accounted for the leak in the pushrod stroke estimation.

Experiments were conducted on a test bench at Texas A&M University. The diagnostic prototype system consisted of a data-acquisition system which interfaces with the truck brake system test bench in the laboratory at Texas A&M University and a desktop computer. Tests conducted of the prototype diagnostic system on the test bench indicated that the prototype diagnostic system accurately predicts the “severity” of the leak (characterized by the “effective area” of the cross-section of the leak) and reasonably predicts the pushrod stroke in the presence of leaks.

The underlying algorithms required the development and corroboration of a mathematical model for pressure transients in the presence of a leak. The model used orifice equations for describing the mass flow rate of air leaking and incorporated the balance of mass equation. The mathematical model was successfully corroborated by the experiments. Measurements of supply pressure, treadle valve plunger displacement and leak mass flow rates are utilized to develop the model. The model has been developed in compliance with current FMCSA and FMVSS norms for brake systems in trucks. All input data to the model are obtained during a full brake application with a supply pressure of 90 psi (722 kPa). The brake system configuration investigated comprised of a front brake chamber directly connected to the primary delivery port of the treadle valve. Controlled amounts of leak were introduced using a flow control valve. A “master” leak data set was obtained with the help of leak flow measurements.

An empirical relationship for mass flow rate of leak was developed with supply pressure and area of leak as independent variables. This empirical relation was fitted with the measurements and an “effective area” of leak was estimated. The effective area of leak and the empirical relation were then input to the previously developed “fault-free” model to obtain the pressure transients in the presence of leaks. To simulate “realistic” leaks, flow control orifices of known diameters were employed to introduce leaks in the system. From measured steady state pressures in the brake chamber, effective area of leak was estimated by “looking up” the “master” leak data set.

Numerical schemes for estimation of push rod stroke under no leak conditions and in the presence of leaks have also been developed. The scheme involving transition detection from mode 2 (phase where the clearance between the brake pads and the drum is overcome) to mode 3 (subsequent deformation of the mechanical components till steady state pressure is attained) has

been found computationally viable. The measured steady state pressures in the brake chamber, treadle valve plunger displacement are utilized to develop the estimation scheme. This scheme can be implemented with the “fault-free” model (no-leak condition) as well as the “leak” model for estimating the push rod strokes under no leak conditions and in the presence of leaks respectively. The estimation scheme developed were successfully implemented using a desktop computer and is amenable for integration onto a prototype hand-held diagnostic device.

7. Investigator Profile

Dr. Swaroop Darbha, the Principal Investigator on this project, is an Associate Professor in the Mechanical Engineering Department at Texas A&M University, College Station, Texas.

He can be contacted at:

320 Engineering/Physics Building Office Wing,
Department of Mechanical Engineering,
Texas A&M University,
College Station,
Texas - 77843-3123
Phone: 979-862-2238
Fax: 979-845-3081
Email: dswaroop@tamu.edu

References

- [1] S. F. Williams and R. R. Knipling. *Automatic slack adjusters for heavy vehicle air brake systems*. Report No. DOT HS 807 724, National Highway Traffic Safety Administration, Washington, D.C., February 1991.
- [2] *Front wheel brake safety facts*. Department of Transportation, Federal Highway Administration, Washington, D. C., USA, 1987.
- [3] *Motor vehicle safety standard no. 121: Air brake systems*. Code of Federal Regulations, Title 49, Part 571, Section 121, October 2003.
- [4] *EC series electric cylinders: Users manual*. PN CUS10050, Version 1.0, Industrial Devices Corporation/Danaher Motion, Rockford, Illinois.
- [5] *B8501: Brushless analog position control manual supplement*. PN PCW-4712, Rev. 1.01, Industrial Devices Corporation/Danaher Motion, Rockford, Illinois, June 1995.
- [6] *B8001 brushless servo drive: Operators manual*. PN PCW-4679, Rev. 1.5, Industrial Devices Corporation/Danaher Motion, Rockford, Illinois, May 1998.
- [7] *IDC Servo Tuner: Operators manual*. P/N PCW-4710, Rev. 1.00, Industrial Devices Corporation/ Danaher Motion, Rockford, Illinois, April 1995.
- [8] *PCI E series user manual: Multifunction I/O devices for PCI bus computers*. National Instruments, Austin, Texas, July 2002.
- [9] Mead Fluid Dynamics, “*Dyla-trol flow controls*,” <http://www.mead-usa.com/products/detail.aspx?id=4>, accessed May 2008.
- [10] All Sensors Corporation, “*Miniature amplified low pressure sensors*,” [http://www.allsensors.com/datasheets/industrial temp/min amp low prime.pdf](http://www.allsensors.com/datasheets/industrial%20temp/min%20amp%20low%20prime.pdf), accessed May 2008.
- [11] S.C. Subramanian. *A Diagnostic System for Air Brakes in Commercial Vehicles*, Ph.D. Dissertation. Texas A&M University, College Station, USA, 2006.
- [12] Shankar C.Subramanian, Swaroop Darbha, and K. R. Rajagopal. *Modeling the pneumatic subsystem of an S-cam air brake system*. Journal of Dynamic Systems, Measurement and Control, American Society of Mechanical Engineers, vol. 126, pp. 3646, March 2004.
- [13] M. Saad, *Compressible fluid flow* 2nd ed., Prentice~ Hall, Englewood Cliffs ,NJ, 1993.
- [14] M. Nyberg and A. Perkovic, “*Model based diagnosis of leaks in the air-intake system of an SI-engine*,” SAE spec publ, SAE, Warrendale, PA, (USA), Feb 1998., vol. 1357, pp. 25–31, 1998.

[15] R.W. Miller, *Flow Measurement Engineering Handbook*, p. 5.5, McGraw-Hill Professional, 1996.

[16] McMaster-Carr, "*Flow control orifices, catalog p471*," <http://www.mcmaster.com/>, accessed May 2008.